Linking patterns of physical and chemical organic matter fractions to its lability in sediments of the tidal Elbe river

Zander, F.; Comans, R.N.J.; Gebert, J.

DOI
10.1016/j.apgeochem.2023.105760

Publication date
2023

Document Version
Final published version

Published in
Applied Geochemistry

Applied Geochemistry 156 (2023) 105760

Contents lists available at ScienceDirect

Applied Geochemistry

journal homepage: www.elsevier.com/locate/apgeochem

Linking patterns of physical and chemical organic matter fractions to its lability in sediments of the tidal Elbe river

F. Zander [a], R.N.J. Comans [b], J. Gebert [a,*]

[a] Delft University of Technology, Department of Geoscience & Engineering, Section Geo-Engineering, Stevinweg 1, 2628 CN Delft, the Netherlands
[b] Wageningen University & Research, Department of Environmental Sciences, Chair Group Soil Chemistry and Chemical Soil Quality, Droevendaalsesteeg 3, 6708 PB Wageningen, the Netherlands

ARTICLE INFO

Editorial handling by: Joyanto Routh

Keywords:
Sediment organic matter
Anaerobic and aerobic degradability
Chemical and physical DOM and SOM fractions

ABSTRACT

Degradability of organic matter in river sediments differs in relation to origin and age. In order to explain previously observed spatial patterns of organic matter degradability and stabilization, this study investigated sediment organic matter (SOM) properties along a tidal Elbe river transect using dissolved organic matter (DOM) fractions, density fractions, carbon stable isotopes and thermometric pyrolysis (Rock-Eval 6©). These properties were linked to SOM decay rates and biological indicators such as chlorophyll *a* and silicic acid in the water phase, and sediment-bound extracellular polymeric substances (EPS), microbial biomass and oxygen consumption. Sediment source gradients were established using the concentration of Zn in the fraction < 20 μm as proxy.

The specific Zn concentration showed that the most upstream location was nourished primarily by upstream fluviatile sediments while the other locations carried a downstream signature. The upstream location was also characterised by the highest concentrations of chlorophyll *a*, microbial biomass, silicic acid, EPS, humic acids and hydrophilic DOM, the most negative $\delta^{13}C$ signature and by the highest oxygen consumption rate, with decreasing trends towards downstream locations. This trend was also evident in the decreasing SOM lability from upstream to downstream, an increasing share of total SOM found in the acid-base-extractable fractions and a decreasing share of carbon in the light density fractions. Thermometric pyrolysis revealed the highest H-index (easily degradable SOM) for the most upstream location and the ratio of the I-index (immature SOM) to the R-index (refractory SOM) to correlate positively with measured SOM decay rates.

This study suggests that spatial patterns of SOM degradability can be explained by a source gradient, with young organic matter entering the system from upstream from predominantly biogenic sources, while downstream sources (North Sea sediment) deliver more refractory SOM that is stabilized in organo-mineral associations to a higher extent. In the investigated sediments, dissolved organic matter represented 0.23–1.20% of the total organic carbon (TOC) from anaerobically degradable SOM, while 4.10–11.46% TOC was liberated as CO_2 and CH_4 after long-term incubation (250 days). Thermometric pyrolysis is shown to serve as a useful proxy for SOM degradability in river sediments, with the Hydrogen-Index (HI) correlating well with degradability and the relationship between the I-index and R-index changing consistently towards lower I-indices and higher R-indices with an increasing degree of SOM stabilization.

1. Introduction

Estuarine sediment organic matter (SOM) originates from a variety of sources, and includes autochthonous organic matter from primary production, allochthonous organic matter from the erosion of floodplain topsoils in the upstream catchment area, marine organic and rural, metropolitan or industrial inputs from wastewater discharge or surface runoff. While it is known that most of the soluble products from organic matter hydrolysis in marine and inland waters, generally summarized as dissolved organic matter (DOM), are highly degradable and consumed within days after production (Dittmar, 2015; Catalán et al., 2016; Ward et al., 2017), the long-term stabilization and mineralisation of the remaining, less degradable organic fraction is less understood. In order to advance understanding of the carbon balance along the river continuum (Vannote et al., 1980), it is therefore of interest to research possible mechanisms of sediment organic matter stabilization and to

* Corresponding author.
E-mail addresses: f.zander@tudelft.nl (F. Zander), rob.comans@wur.nl (R.N.J. Comans), j.gebert@tudelft.nl (J. Gebert).

https://doi.org/10.1016/j.apgeochem.2023.105760
Received 8 April 2023; Received in revised form 21 July 2023; Accepted 29 July 2023
Available online 2 August 2023

find proxies to assess its lability.

Next to its role in the global carbon cycle and its eco-functionality (Hoffland et al., 2020), SOM influences sediment properties that are relevant for the navigability of ports and waterways, such as rheological characteristics (Wurpts and Torn, 2005; Shakeel et al., 2019, 2021) or settling and consolidation behaviour (Sills and Gonzalez 2001; Jommi et al., 2019). A multitude of studies have investigated SOM quality and stability in terrestrial soils, but only few studies have attempted to link SOM quality proxies to SOM turnover in freshwater sediments (Bastviken et al., 2003; Gebert et al., 2006) or recent alluvial sediment deposits (Kobierski and Banach-Szott, 2022). However, recent research has demonstrated the applicability of amino acid and amino sugar ratios and their normalization to TOC to infer the changes in organic matter sourcing and degradation status (Wei et al., 2021; Ankit et al., 2022).

Lehmann and Kleber (2015) described soil organic matter as a continuum of progressively decomposing organic compounds. In terrestrial soils, the classification of organic matter quality and its degradability has been approached by various methods of chemical and physical fractionation, as reviewed by Von Lützow et al. (2007). Helfrich et al. (2007) and Shen et al. (2018), for example, used chemical fractionation to isolate stable soil organic matter from different agricultural and forest soils and to assess the influence of different land uses on the organic matter quality and quantity of soils. Kögel-Knabner and Rumpel (2018) reviewed molecular methods to elucidate organic matter properties. Hoffland et al. (2020) concluded that in terms of the eco-functionality of organic matter in soils, especially the non-degradable (recalcitrant) fraction of organic matter is under-researched.

For sediments, Gebert et al. (2006) found that maximum anaerobic SOM decay rates in ten fluviatile sediments correspond to the amount of carbon in the light density fraction (< 1.4 g cm^{-3}). Wakeham and Canuel (2016) identified organic matter in riverine delta sediments to not be evenly distributed across density fractions, with the biggest share of SOM (approximated by total organic carbon) in the meso-density fraction (1.6–2.5 g cm^{-3}). Grasset et al. (2021) showed that the extent of methane production could be well predicted by the quantity of particulate organic matter and its quality, the latter assessed by the ratio of total organic carbon (TOC) to total nitrogen (TN). Zander et al. (2020) reported pronounced spatial gradients of SOM degradability in the tidal freshwater transect through the Port of Hamburg, which correlated with patterns of ^{13}C enrichment and an increased share of total organic carbon (TOC) in the heavy density fraction.

The study at hand further investigates the source and age gradient of organic matter by linking the physical and chemical SOM and DOM fractions to SOM degradability and biotic and abiotic sediment properties. The investigated transect in the freshwater tidal Elbe River covers rural, metropolitan and industrial areas, and hence OM inputs from soil erosion, from primary production, from anthropogenic and industrial sources (effluents, surface run-off) and from near-bed transport of North Sea sediment due to tidal pumping (Schwartz et al., 2015). SOM degradability (lability) is defined as the share of carbon released by microbial degradation under aerobic or anaerobic conditions with respect to TOC.

It was hypothesized that

1. SOM lability along the investigated transect depends on SOM origin and age: fresh planktonic, easily degradable biomass feeds organic matter stocks from upstream while less degradable organic matter is older and stabilized in organo-mineral complexes. These can form in situ as a result of progressive SOM degradation (ageing) or are as such imported from sources like eroded upstream and downstream alluvial soils and from North Sea sediment.
2. SOM chemical (e.g. hydrophilics, humic and fulvic acids) and physical fractions (e.g. density fractions) reflect in biological SOM degradation kinetics.
3. Concentrations of dissolved organic matter (DOM) in the sediment's pore water reflect SOM degradability.
4. With progressive SOM decay, the mass of sediment present in the light density fractions decreases and δ^{13}C values of the bulk sediment increase. These patterns mirror the spatial trend of SOM degradability along the investigated transect.

Zander et al. (2020) provide a first data set regarding the spatial gradients of SOM degradability. The study at hand focuses on gradients of organic matter quality described SOM fractions, both in situ and in SOM degradation experiments, and their relation to SOM degradability, and the observed changes in thermometric indices (Rock-Eval 6©), carbon stable isotopes and density fractions. SOM degradability is interpreted with respect to the short- and medium time frame (days, years).

2. Materials and methods

2.1. Investigation area and sampling approach

Sediment samples for this study were collected from different locations along a transect of around 30 river kilometres (P1 = river km 616, P9 = river km 646, Fig. 1) through the Port of Hamburg (site description in Zander et al., 2020) using 1 m core sampler ('Frahmlot'). On board, the core was divided into three layers based on differences in visual consistency and strength: fluid mud (FM), pre-consolidated sediment (PS), and consolidated sediment (CS), from top to bottom.

In this study, samples from the locations P1, P2, P6, P8 and P9 were analysed for SOM fractions. Sample selection was based on differences in location, depth and measured SOM degradability. Samples from additional locations were analysed for further physicochemical and biological parameters, including extracellular polymeric substances (EPS), microbial biomass, carbon stable isotopes, Rock-Eval pyrolysis, aerobic and anaerobic SOM decay rates, silicic acid in the pore water, and chlorophyll in the water column.

2.2. Standard properties of solids and pore water

The analysis of solids properties included total nitrogen (TN, DIN EN 16168), total organic carbon (TOC, both DIN ISO 10694), water content (WC, DIN ISO 11465), redox potential (Eh, DIN 38404), particle size distribution (DIN ISO 11277), oxygen consumption after 3 h from SOM degradation (AT3h, TV-W/I 1994), phosphorus (P) and sulphur (S, both DIN ISO 11885), pH-value (pH, DIN EN 15933) and electrical conductivity (EC, DIN EN 27888). The following parameters were measured in filtrated pore water: dissolved organic carbon (DOC, DIN EN 1484), ammonium (NH_4^+, DIN ISO 11732), phosphate (PO_4^{3-}, DIN ISO 6878), sulphate (SO_4^{2-}, DIN ISO 10304), and silicic acid (as SiO_2, DIN 38405-D21:1990–10). The concentration of Zn in the particle size fraction < 20 μm was used as a proxy of the share of upstream sediment in the total sediment mixture (Groengroeft et al., 1998). Here, the particle fractions were separated by sieving and sedimentation analysis (DIN ISO 11277) and Zn analysed in the size fraction < 20 μm (medium silt and finer) after aqua regia digestion by atomic absorption spectroscopy (AAS).

2.3. Organic matter fractions

Water- and acid-base-extractable SOM fractions were analysed on a subset of 16 samples collected in 2018 (for properties, see Table 1). We use water-extractable SOM to approximate the DOM fraction of these sediments. Neutral water extracts reflect the properties of dissolved natural organic matter (Olk et al., 2019), while we have used a high and constant sediment to water ratio of 1:2 for all samples to reduce dilution relative to pore water as much as possible. Organic matter was extracted on two aliquots using firstly, a water extracted (ratio sediment to water was 1:2) and, secondly, a sequential acid-base-extraction (procedures described in detail in Van Zomeren and Comans, 2007). This acid-base

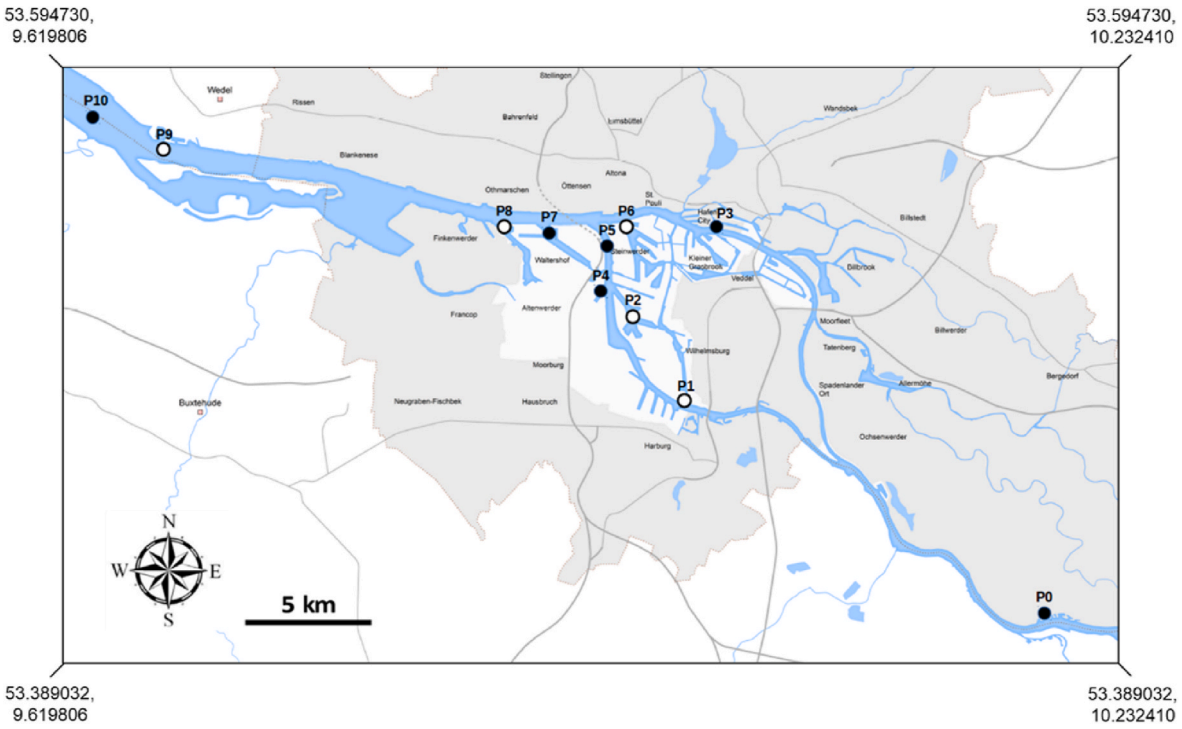

Fig. 1. Investigation area around the Port of Hamburg (adapted from Hamburg Port Authority) with sampling locations between river km 598 (P0, upstream) and 646 (P10, downstream). White circles represent the sampling locations investigated in this study. Coordinates refer to WGS84.

Table 1
Selected abiotic and biotic sediment properties of samples investigated in this study W1 to W16 = sample ID.

Location	W1	W2	W3	W4	W5	W6	W7	W8	W9	W10	W11	W12	W13	W14	W15	W16
	P1	P1	P1	P1	P2	P2	P2	P6	P6	P6	P6	P6	P6	P9	P9	P9
Sampling date	09/18	09/18	11/18	11/18	11/18	11/18	11/18	08/18	08/18	09/18	09/18	11/18	11/18	09/18	11/18	11/18
Layer	PS	CS	PS	CS	FM	PS	CS	PS	PS	PS	CS	PS	CS	CS	PS	CS
Depth b.l. (cm)	0–15	15–50	0–20	20–50	0–10	10–40	40–80	0–20	20–35	0–20	20–45	0–30	30–70	25–50	10–30	30–65
TN (% DM)	1.0	0.9	0.8	1.0	0.4	0.5	0.5	0.4	0.4	0.4	0.4	0.4	0.4	0.2	0.2	0.2
TOC (% DM)	6.6	6.7	5.7	6.8	3.8	3.9	3.9	3.5	3.6	3.1	3.3	3.1	3.3	1.8	1.8	1.8
TOC/TN (%/%)	7	7	7	7	9	8	8	8	8	8	8	9	8	11	11	11
DOC (mg/l)	30	25	21	39	1	15	22	18	26	25	30	12	30	30	8	
Degradable AN (%)	24	20	16	14	15	14	12	24	19	16	11	50	12	9	13	19
Clay,< 2 µm (%)	45	47	48	38	48	46	51	43	44	38	41	38	34	16	15	16
Silt, 2–63 µm (%)	47	45	48	56	46	48	39	47	48	37	46	45	45	26	29	34
Sand, > 63 µm (%)	8	7	4	7	6	7	10	9	8	25	13	18	21	58	56	50
(Clay + Silt)/TOC	14	14	17	14	25	24	23	26	25	24	26	27	24	23	24	28
WC (% DM)	520	393	408	362	321	278	242	295	260	265	235	242	192	95	115	103
Eh (meV)	−250	−220	−280	−240	−190	−260	−300	−310	−300	−260	−290	−140	−280	−265	30	−60
pH	7.1	6.7	7.2	6.6	7.4	7.4	7.1	7.4	7.4	7.4	7.3	7.4	7.3	7.3	7.4	7.3
LF (% DM-bulk)	40	51	43	53	24	24	25	35	19	18	26	24	27	8	7	8
HF (% DM-bulk)	60	49	57	47	76	76	75	65	81	82	74	76	73	92	93	92

b.l. = below lutocline, DM = dry matter, FM = fluid mud, PS = pre-consolidated sediment, CS = consolidated sediment, TN = total nitrogen, TOC = total organic carbon, DOC = dissolved organic carbon in pore water, Degradable AN = anaerobically degradable SOM, WC = water content, Eh = redox potential, LF and HF = light and heavy density fraction.

fractionation method uses aggregation/precipitation and dissolution properties of natural organic matter established by the International Humic Substances Society (IHSS) to determine acid-base-extractable DOM humic acid (HA), fulvic acid (FA), hydrophobic neutrals (HoN) and hydrophilic acids (Hi) as described in Straathof et al. (2014). Although hydrolysis of ester groups in natural organic matter may occur during alkaline extraction, the extent remains limited within 24 h extraction time under a N_2-atmosphere (Olk et al., 2019), in accordance with the applied procedure of Van Zomeren and Comans (2007).

In brief, the starting solution of the total extracted DOC was acidified to pH 1 using 6 M HCl, the acidified solution was then centrifuged, separating the HA from the supernatant. The pellet of HA was re-dissolved in a base solution of 0.1 M KOH and subsequently measured as DOC on a Segmented Flow Analyser (SFA; Straathof et al., 2014), while the remaining supernatant was then equilibrated with the resin DAX-8 (SigmaAldrich) for 1 h at 220 rpm horizontal shaking at a 1:5 resin to solution ratio. This equilibration step pulled FA and HoN compounds out of solution by binding them to the surface of the

hydrophobic resin. The compounds that remained in solution are operationally defined as hydrophilic acids and their concentration was measured as DOC on an SFA. Finally, the resin separated from the Hi fraction was equilibrated in 0.1 M KOH, re-dissolving the FA pool. The concentration of FA was also measured as DOC on an SFA while the concentration of the remaining HoN pool was calculated by determining the proportion of the DOC which was not re-dissolved from the resin (as it remains bound to the resin even under alkaline conditions).

The recovery rate was between 78% and 87% for the acid-base-extraction and 80%–97% for the water-extraction. For both extractions, the fractions have been normalised to 100% recovery relative to total DOC.

2.4. Density fractions

The procedure is based on the method first presented by Van den Pol-van Dasselaar and Oenema (1999), adapted from Meijboom et al. (1995), and also applied by Gebert et al. (2006) on riverine sediments in a previous study. The samples were placed in glass beakers, mixed with an excess of LUDOX® HS-40 colloidal silica suspension in water (Sigma-Aldrich) with a cut-off density of 1.4 g cm^{-3} and stirred thoroughly. Light material < 1.4 g cm^{-3} accumulated at the surface and was separated from heavy material > 1.4 g cm^{-3}, sinking to the bottom, by decantation. The two fractions were washed with distilled water and oven-dried at 105 °C for subsequent physical and chemical analyses (see Section 3.3). More details are given in Zander et al. (2020).

2.5. Carbon stable isotopes

The $\delta^{13}C$-values of the sediment organic matter were determined on bulk fresh and incubated samples, using an isotope-ratio mass spectrometer (Delta V; Thermo Scientific, Dreieich, Germany) coupled to an elemental analyser (Flash 2000; Thermo Scientific). Prior to analysis, samples were treated with phosphoric acid (43%, 80 °C for 2 h) to release inorganic carbon. Values are expressed relative to Vienna Pee Dee Belemnite (VPDB) using the external standards IAEA IAEA-CH7 (−32.15‰ vs. VPDB) and IVA soil 33802153 (−27.46‰ vs. VPDB). Standards were measured every 10 samples, standard deviation was 0.09 and 0.12, respectively. Analytical replicate precision was < 0.2‰.

2.6. Degradation of organic matter

The sediment samples collected from the different layers (section 2) were stored in their gas-tight containers in a refrigerator at 4 °C in dark until analyses commenced, typically within a few days of sample collection. SOM decay was assessed by measuring carbon release into the gas phase (bottle headspace) over time upon incubation of the samples in the laboratory in closed glass bottles sealed with butyl rubber stoppers under anaerobic and aerobic conditions for more than 250 days (see also Zander et al., 2020). Visible benthic macrofauna was removed before incubation, if present at all. All samples were analysed in triplicate at their in situ water content.

2.6.1. Anaerobic degradation of organic matter

Depending on the water content and the expected gas production rate, about 150–300 g of fresh sample were placed into 500 ml glass bottles. The bottle headspace was flushed with 100% N_2 to establish anaerobic conditions and incubated at 36 °C in dark. The elevated experimental temperature was chosen to warrant exhaustive decay of organic matter within the time frame of the experiment (see Fig. 2) in order to assess degradability of sediment organic matter as accurately as possible.

For some samples, measurements were carried out for at least 500 days until cumulative carbon release approximated a plateau, i.e., decreased to very low rates. The total amount of generated gas was expressed as mass unit of carbon released per mass unit of organic carbon as present in the original sample. Gas chromatographic analyses did not detect any other gases besides N_2, CH_4, and CO_2. The total number of original samples analysed for anaerobic SOM degradability equalled n = 268.

2.6.2. Aerobic degradation of organic matter

Aerobic SOM decay was quantified at an incubation temperature of 20 °C. To determine the degradation of organic matter under aerobic (i.e. oxic) conditions, 15 g of homogenised fresh sample was incubated in 1 l glass bottles at 20 °C in the dark with a headspace of atmospheric air. The sample was distributed at the bottom of the bottles in a layer of only a few millimetres thickness in order to minimise limitations to the diffusion of oxygen into the sample.

The bottle headspace was flushed with atmospheric air in the beginning of the measurements. The generation of CO_2 was calculated from the increase in headspace CO_2 concentration, measured with gas

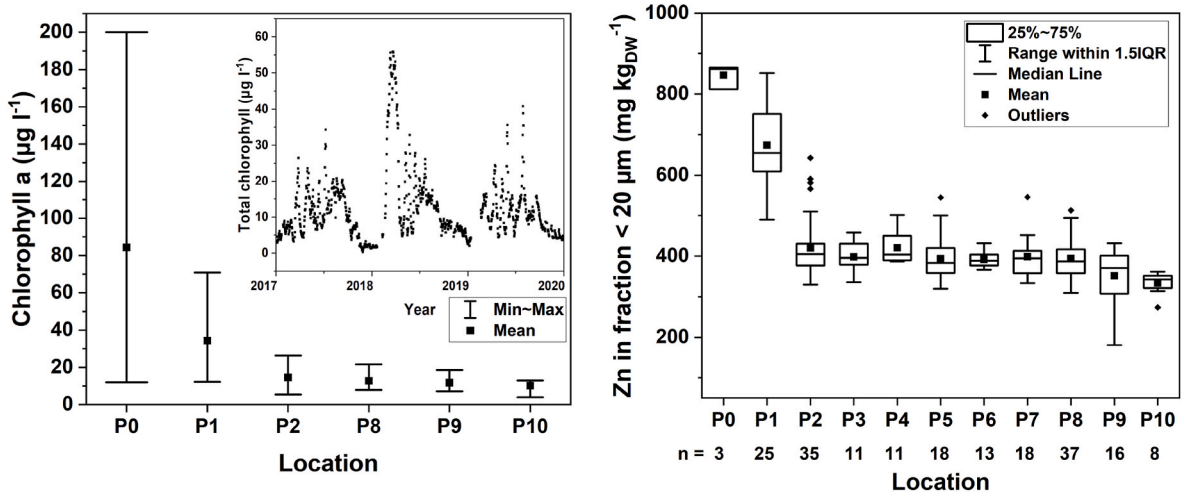

Fig. 2. Left: in situ chlorophyll concentration in the water column from upstream (P0) to downstream (P10) in 2018 (n = 5). Squares = average values, error bars = maximum, minimum. Data for P0 and P10: FGG Elbe data portal (2020), total chlorophyll concentration from 2017 to 2020 (small Figure): Hamburg Serviceportal (2020), near location P8. Right: concentration of Zn in the particle size fraction < 20 µm along the investigated transect for PS and CS layers from 2018 to 2019, P0 = river-km 579, P10 = river-km 646.

chromatographic analyses (GC-TCD, Da Vinci Laboratory Solutions). As soon as a concentration of 2.5% CO_2 in the bottle headspace was reached, the bottle was flushed anew with atmospheric air, then measurements were resumed. Besides O_2, N_2 and CO_2, no other gases were detected. The total number of original samples analysed for aerobic SOM degradability equalled n = 243 for aerobic samples.

2.6.3. Analytical details

Headspace pressure was measured manually with a pressure gauge (LEX1, Keller) using a needle pierced through the stopper. The generation of CH_4 and CO_2 (anaerobic) or only CO_2 (aerobic) was calculated from the (increase in) headspace pressure in combination with gas chromatographic analyses (GC-TCD, Da Vinci Laboratory Solutions) of headspace composition (CH_4, CO_2, O_2, N_2) using the ideal gas law. Extraction of headspace volume for GC sampling was corrected for in the calculation of gas generation and respiratory CO_2 release by measuring the headspace pressure before and after sampling. All values are reported as the sum of (CH_4-C and) CO_2-C measured in the gas phase and the share of CO_2-C dissolved in the aqueous phase. The latter was calculated using the CO_2 concentration, the volume of water, the pressure in the bottle headspace and the temperature-corrected solubility of CO_2 in water as given by Henry's constant (given in Sander, 2015). The frequency of measurements was adapted to the gas production and the respiration rates and decreased from daily intervals at the beginning of the incubation to monthly intervals at the end.

The average deviation of maximum and minimum values of the cumulative carbon release of triplicate incubations from their average was < 5%.

2.6.4. Incubation temperature

As decay rates are lower under anaerobic than under aerobic conditions, an elevated temperature was chosen for the anaerobic incubation (36 °C versus 20 °C during aerobic incubation) to enable similar incubation time scales. The response of aerobic and anaerobic SOM decay to temperature was analysed by measuring SOM decay for > 250 days on aliquot samples incubated at 5, 10, 20, 28, 36 and 42 °C in the same way as described above. In order to directly compare SOM decay under anaerobic and aerobic conditions, anaerobic SOM decay rates were normalised to a temperature of 20 °C based on data from this separate temperature experiment (Zander, 2022). Hereby, the temperature coefficient function $Q_{16} = R_2/R_1$ was used, with R_1 and R_2 as the cumulative released carbon at the given temperature at the respective time of incubation (i.e., R_1 at 20 °C and R_2 at 36 °C).

2.6.5. Organic matter decay rates

The detailed description of the methods to measure aerobic and anaerobic organic carbon release and to calculate the corresponding decay rates can be found in Zander et al. (2022). In brief, the time course of cumulative carbon release (CH_4-C and CO_2-C) was described by one phase or two phase exponential decay fits (OriginPro2019). These multi-phase models follow the approach of the multi-G model used by Westrich and Berner (1984), reviewed by Arndt et al. (2013) for phytoplankton decay, where organic matter is split up into classes of individual compounds with separate decay rate constants (k). Two phase functions were split into two single functions with different organic matter decay kinetics. For each function, the organic matter decay rate (mg C g_{TOC}^{-1} d^{-1}) was obtained from the derivative of the sum function. The daily decay rates were calculated from the derivative of the exponential fit of the cumulative curve.

2.6.6. Response of anaerobic SOM decay and SOM fractions to different temperatures

Temperature sensitivity experiments were performed to quantify differences in SOM decay rates and the corresponding extractable SOM fractions in relation to temperature for aerobic and anaerobic conditions. To this end, sediment samples from a long term (> 800 days) experiment, where aliquots of the same sediment sample (location P7) had been incubated at different temperatures between 5 and 42 °C (Zander, 2022), were analysed to quantify water- and acid/base-extractable SOM fractions.

2.7. Rock-Eval 6© pyrolysis

The Rock-Eval 6© method was used to further characterise SOM, especially the share of hydrocarbon and oxygen bearing components. In brief, the sample is first pyrolysed and subsequently oxidized, both steps using a temperature ramp, and the resulting release of hydrocarbons, CO and CO_2 are quantified with a flame ionisation and infrared detector. The method is described in detail Sebag et al. (2016) and Oliveira et al. (2017). In brief, analyses were carried out with 30–100 mg of powdered samples using a Rock-Eval 6© pyrolyzer manufactured by Vinci Technologies. Phase one was a pyrolysis in an inert N_2 atmosphere starting at a temperature of 200 °C until 650 °C with a heating rate of 25 °C/min, phase two included thermal decomposition in an oxidized atmosphere starting at a temperature of 400 °C until 850 °C with the same heating rate (Sebag et al., 2016). The Hydrogen-index (HI), a proxy for more labile organic matter, was calculated by integrating the amounts of hydrocarbons normalised to the amount of total organic carbon (Lafargue et al., 1998). The I-index, assessing the preservation of thermally labile immature organic fraction and the R-index, assessing the contribution of thermally stable refractory organic fraction corresponding to the most persistent or refractory SOM fraction were defined by Sebag et al. (2006, 2016).

2.8. Extracellular polymeric substances (EPS)

All analyses were performed in triplicates. 0.14 M NaCl was used as negative control in triplicate. All reactions were measured three times. For the determination of proteins, carbon hydrates and uronic acids standard curves were established by performing the respective assay on dilution series of a standard solution of known concentration in triplicates.

Total EPS was isolated according to Wingender et al. (2001) with a few modifications. Mud samples were weighed and suspended in sterile 0.14 M NaCl solution (mass ratio of sample wet weight to NaCl solution of 1:16, for samples 19201 to 21206 of 1:10). The mud suspensions were stirred on a magnetic stirrer for 60 min with 200 rpm at room temperature. To remove unsolved particles the suspensions were centrifuged for 30 min at 20,000×g at 10 °C. The decanted supernatants were filtered two times through cellulose acetate membranes (pore diameter, 0.2 μm). Aliquots were stored at −20 °C.

2.9. Microbial biomass

Microbial biomass was determined using the fumigation-extraction method according to Vance et al. (1987; DIN EN ISO 14240-2). Dissolved organic carbon was, quantified with the Total Organic Carbon Analyser TOC-L (Shimadzu). Microbially bound carbon was calculated with the ratio 1:0.38 after Vance et al. (1987).

2.10. Other parameters

Chlorophyll *a* concentration as an indicator for phytoplankton biomass was measured in situ with a CTD probe (CTD90, Sea&Sun, data provided by Hamburg Port Authority) in the near-bottom water column. For the points P0 and P10 (Fig. 1), chlorophyll data were gathered from FGG Elbe data portal (2020), chlorophyll concentration from 2017 to 2020 near location P8 was obtained from Hamburg Serviceportal (2020).

3. Results

3.1. Origin and properties of investigated sediments

Sediment properties across the transect showed strong gradients (Table 1). Location P9 (downstream, samples W14, W15 and W16) showed the *lowest values* total nitrogen (TN), total organic carbon (TOC), anaerobically degradable SOM (Degradable AN), clay, silt, water content (WC), mass% of sediment in the light density fraction (LF), oxygen consumption after 3 h (AT_{3h}) and silicic acid. Upstream location P1 (upstream, samples W1, W2, W3 and W4) showed the *highest* concentrations in TN, TOC, DOC, silt, the highest water content and the highest share of sediment in the light density fraction. The ratio of TOC to TN increased in downstream direction. Downstream locations P6 and particularly P9 were characterized by a higher sand and a lower content in fines. Normalising the content of fines by TOC indicated similar values for sites P2 to P9, with only upstream site P1 standing out with high TOC in relation to the content of fines. Concentrations of dissolved organic carbon

To estimate the shares of upstream and downstream (marine) material in the total sediment mix found at each location, the concentration of Zn in the particle size fraction < 20 µm was used as a proxy, differing significantly between upstream (higher concentrations) and North Sea material (lower concentrations; Groengroeft et al., 1998). High upstream concentrations originate from historic pollution of the Elbe by upstream industrial and municipal effluents, either discharged directly into the Elbe or into Elbe tributaries. Fig. 2 (left) shows that from a downstream point of view the sediments are dominated by (less polluted) North Sea material until Elbe km 619 (P2, 400 mg Zn kg_{DW}^{-1} in fraction < 20 µm), while locations further upstream of this point are characterised by upstream sediments with higher Zn concentration (P1 and P0: 650 and 850 mg Zn kg_{DW}^{-1}). The Zn concentration was similar for pre-consolidated (PS) and consolidated (CS) material. In the water column, the chlorophyll *a* concentration generally decreased from upstream (P0) to downstream (P10, Fig. 2, right). The small figure shows how chlorophyll varies seasonally by example of continuous measurements near location P8 (Hamburg Serviceportal, 2020), indicating a multi-peak algae bloom with generally higher values in the warmer seasons, decreasing towards winter. In 2018, the first peak occurred exceptionally early.

Fig. 3 illustrates clear differences between upstream and downstream sediment properties for the biotic parameters silicic acid, microbial biomass, AT3h and EPS. At downstream locations (i.e. P8 to P10), the lowest concentrations of silicic acid (in pore water), microbial biomass (in sediment), oxygen consumption after 3 h (AT_{3h}, in sediment) and extracellular polymeric substances (EPS, measured in the sediment) were found (Fig. 3). These trends align with the trend of decreasing SOM degradability (Fig. 4), and decreasing shares of water-extractable SOM hydrophilics, increasing shares of water-extractable fulvic acids and hydrophobic neutrals and an increasing ratio of acid-base-extractable to water-extractable hydrophilics (see Fig. S1).

As almost all sediment samples were characterised by negative redox

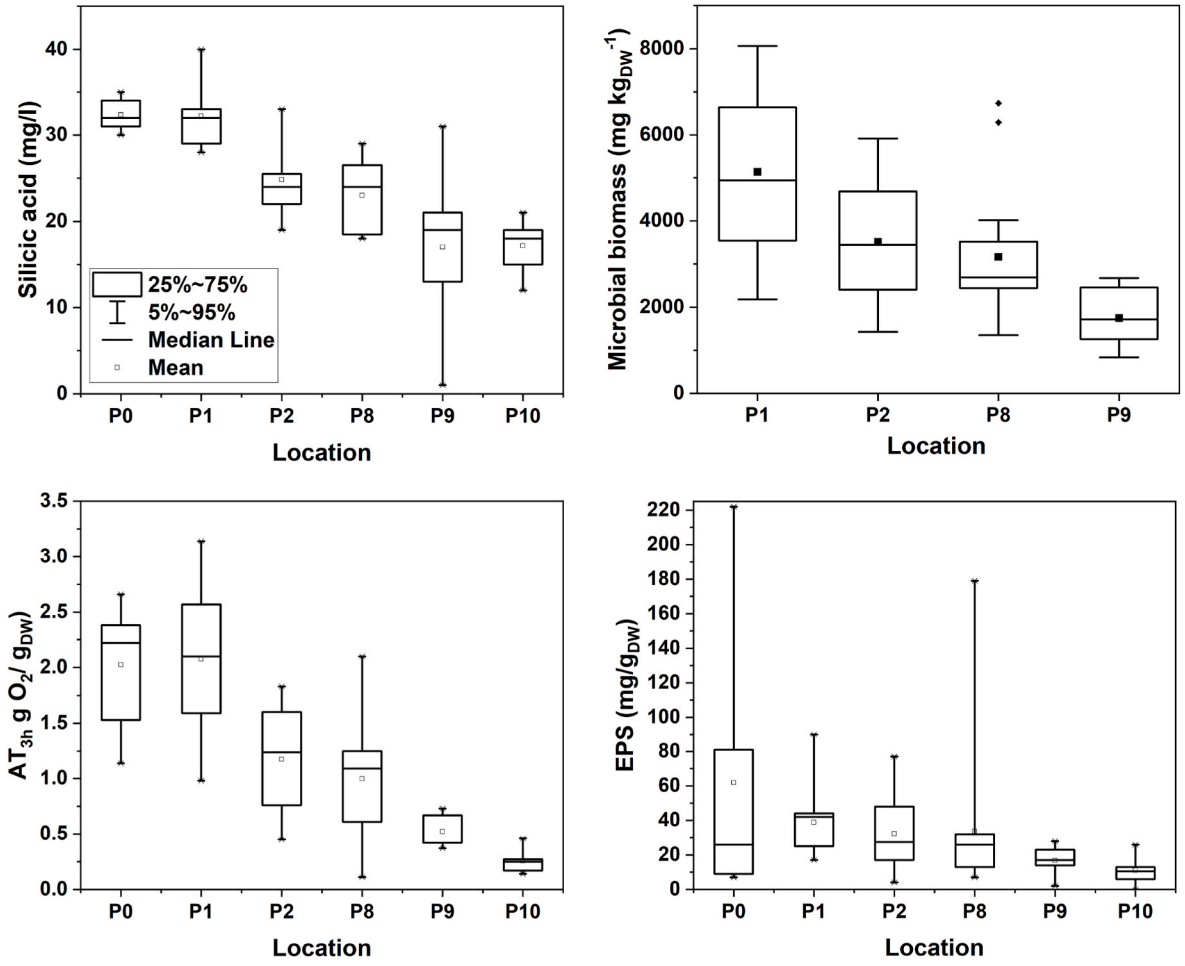

Fig. 3. Silicic acid (SiO_2), microbial biomass, oxygen consumption after 3 h (AT_{3h}) and extracellular polymeric substances (EPS) concentration from upstream (x axis left) to downstream (x axis right), n ≥ 6. Lines = median values, squares = mean values, boxes = 25th and 75th percentile. Part of the data (P1 to P9 from 2018) for silicic acid and oxygen consumption after 3 h are shown in Zander et al. (2020).

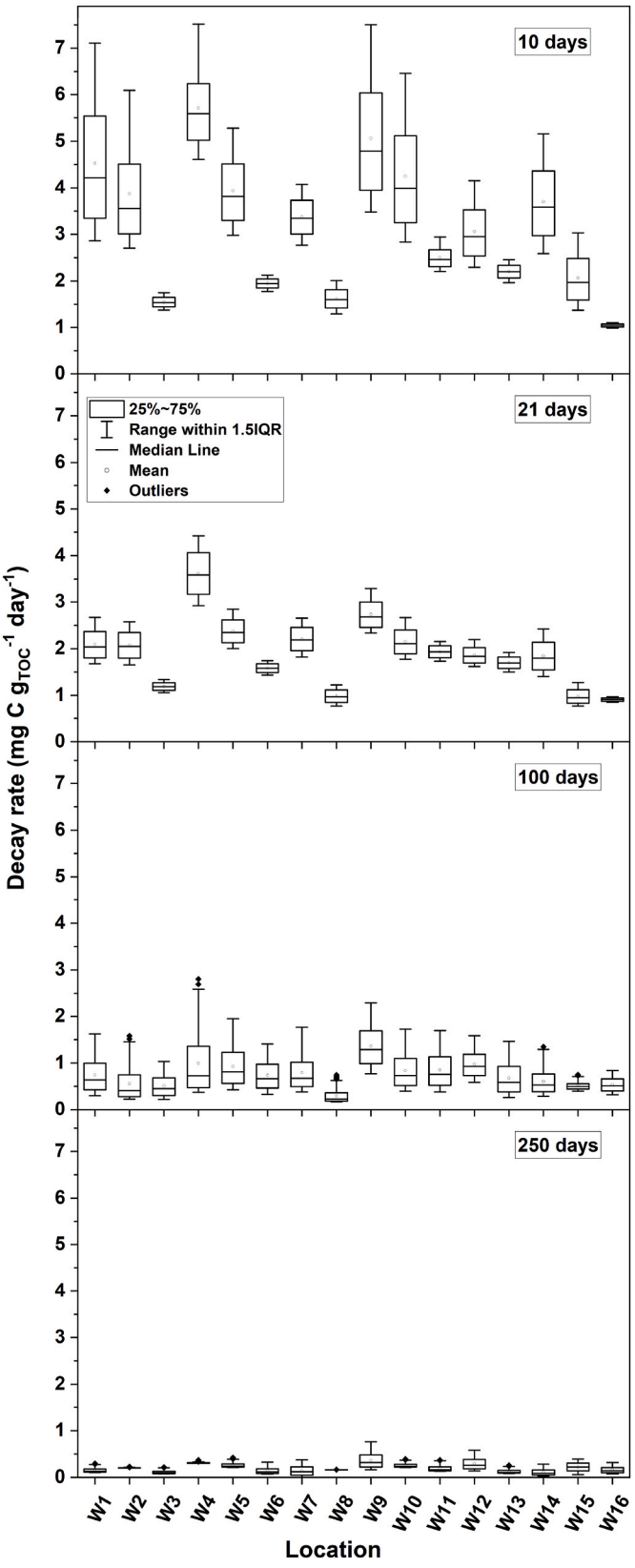

Fig. 4. Anaerobic decay rates for 16 samples of this study (for properties see Table 1), obtained from the first derivation of the cumulative C release over 0-10, 11-21, 22-100 and 101–250 days.

potentials (Table 1), only decay rates for anaerobic SOM degradation were considered in this study. SOM decay rates were obtained from the first derivative of the cumulative C release, as explained in Zander et al. (2022). For short-term decay (within the first 21 days, Fig. 4, upper panel), large differences in decay rates were found between the samples (along the transect), whereas decay rates converged to similar values in the longer term (Fig. 4, lower panel). Site-specific variability of organic matter quality and geochemical boundary conditions affected SOM decay therefore mostly in the initial stages of decay while degradation rates of more stable (less labile) SOM were more similar along the transect.

3.2. Extractable SOM fractions

3.2.1. Field transect

Water-extractable and acid-base-extractable SOM fractions were analysed on a subset of 16 samples from 2018 (for properties, see Table 1). The concentrations of all fractions were found to decrease from upstream to downstream locations in the water-extractable SOM (Fig. 5, left). At all locations, all water-extractable SOM fractions, except for the hydrophobic neutrals (HoN), increased with depth from the upper FM/PS layers to the lower CS layers, this change being most pronounced at upstream locations. For the HoN fraction, this pattern was also found at upstream location P1. With the acid-base extraction, up to 80 mg C g_{TOC}^{-1} of SOM were liberated (Fig. 5, middle column) at location P1, exceeding water-extractable SOM concentrations in all fractions by about one order of magnitude. The spatial and depth-related trends described for the water-extractable fraction were inversed for the acid-base-extractable fraction, increasing from 60 mg C g_{TOC}^{-1} (P1) to 160 mg C g_{TOC}^{-1} (P9).

Humic acids (HA) were the largest contributor to extractable SOM at all locations, making up around 50%–60% of water- and acid-base-extractable SOM. The ratio between and acid-base-extractable and water-extractable SOM (AB/W) increased in downstream direction for all fractions with the exception of the HoN fraction (Fig. 5, right). The ratio between the acid-base fraction and the water-extractable fraction can be interpreted as a dimensionless solid/liquid partitioning coefficient, which was found to be between 5 and 60 for total water-extractable SOM, and the HA and FA fraction. The largest differences in the partitioning coefficients of the SOM fractions between upstream (P1) and downstream (P9) locations were found for the HA fraction (factor 5 to 50) and the Hi fraction (factor 20 to 200). Together, these results indicate an increase in the share of mineral-bound SOM towards downstream and changes in the contribution of individual fractions to total water-extractable SOM along the transect. By the example of material from pre-consolidated (PS) layers, the latter is detailed in Fig. S1.

3.2.2. Effect of temperature and time on anaerobic SOM decay and water-extractable SOM dynamics

Water-extractable SOM fractions were analysed in aliquots of a sediment sample that had been incubated under anaerobic conditions at temperatures between 5 and 42 °C for 865 days. Due to the temperature-dependency of SOM degradation, analysis of SOM fractions from aliquots incubated at different temperatures at the same given point in time allowed to capture different states of degradation of the same original sample. The levelling off of the cumulative SOM decay curve (plateau, see also Zander et al., 2020; Zander et al., 2022), caused by declining degradation rates, was reached earlier at higher incubation temperatures (data not shown). Cumulative C release varied between 13 mg C g_{TOC}^{-1} at 5 °C and 130 mg C g_{TOC}^{-1} at 42 °C (Fig. 6, left, namely, between 1.3% and 13% of TOC.

The total water-extractable SOM and the concentration of the individual fractions increased with increasing incubation temperature (Fig. 6, left). From 5 to 42 °C, the FA fraction increased by a factor of 6, the Hi fraction by a factor of 3 and the HoN fraction by a factor of 2. The concentration of humic acids (HA) also increased, but less consistently.

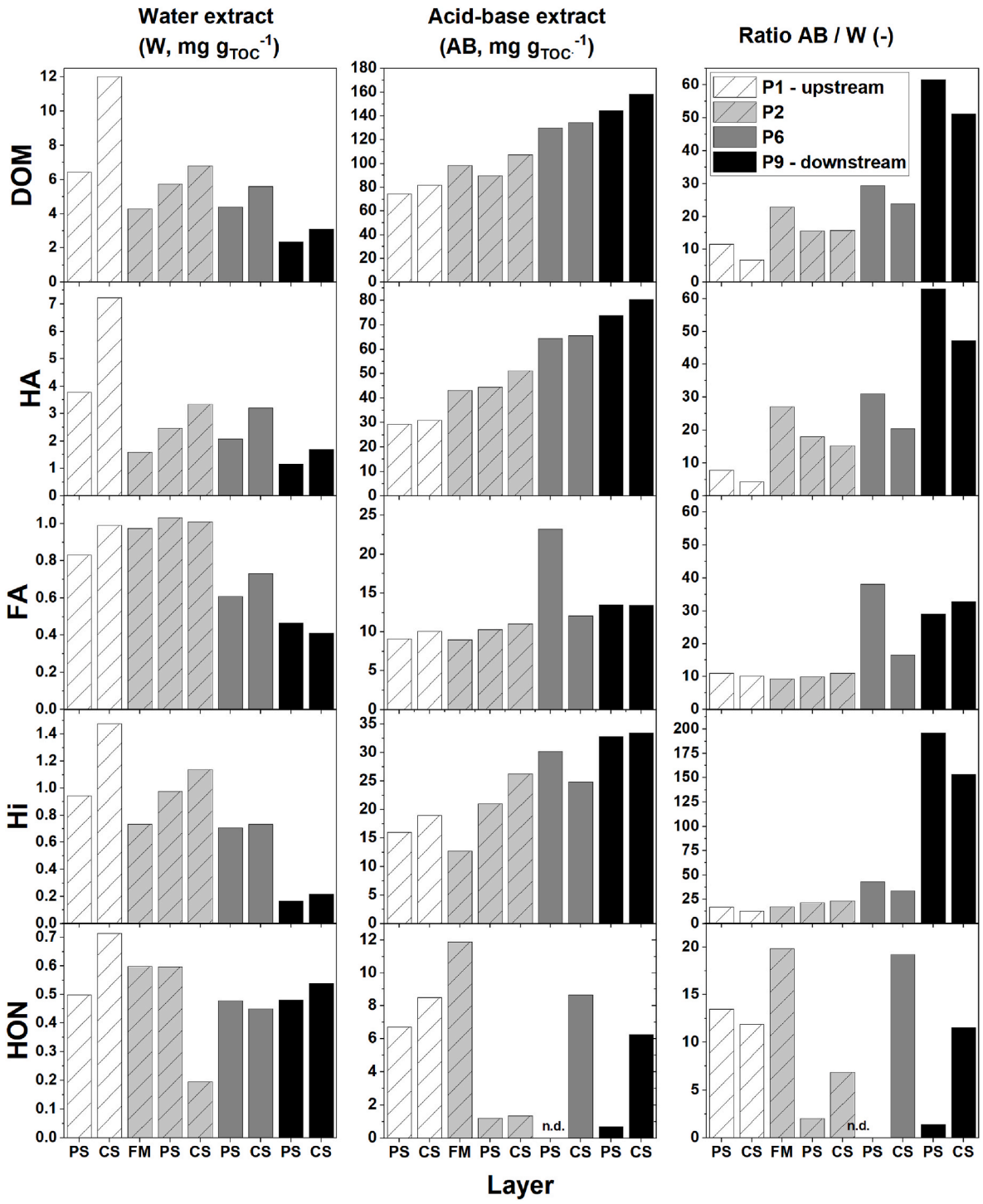

Fig. 5. Water-extractable SOM fractions (left), acid-base-extractable SOM fractions (middle) and ratio between acid-base and water-extractable SOM (right). Total extracted SOM, HA (humic acid), FA (fulvic acid, Hi (hydrophilic acid), HoN (hydrophobic neutrals), concentrations are normalised to total organic carbon (TOC). Observe differently scaled y-axes. n.d. = not determined.

After 865 days of anaerobic incubation at 42 °C, i.e. the temperature yielding the most exhaustive SOM decay, a total of 24.1 mg C g_{TOC}^{-1} were transferred into DOM whereas 130 mg C g_{TOC}^{-1} was transferred into gas phase carbon (CO_2, CH_4). For the other samples analysed in this study (incubated anaerobically for 250 days, Table 1), the values were lower due to the shorter incubation period, namely, between 2.3 and 12 mg C g_{TOC}^{-1} were transferred into DOM and 41.0–114.6 mg C g_{TOC}^{-1} into gas.

The second experiment, investigating the time course of SOM release using a constant incubation temperature (36 °C), showed that concentrations of total water-extractable SOM and the FA, Hi and HoN fractions increased clearly over time of incubation. Total water-extractable SOM increased from 3 to 5 mg C g_{TOC}^{-1} (3–45 days), and total cumulatively degraded SOM from 1 to 16 mg C g_{TOC}^{-1} (Fig. 6, right).

3.3. Density fractions, carbon stable isotopes and thermometric fractions

The share of TOC in the light density fraction was assumed to represent the more easily degradable organic matter (Song et al., 2012).

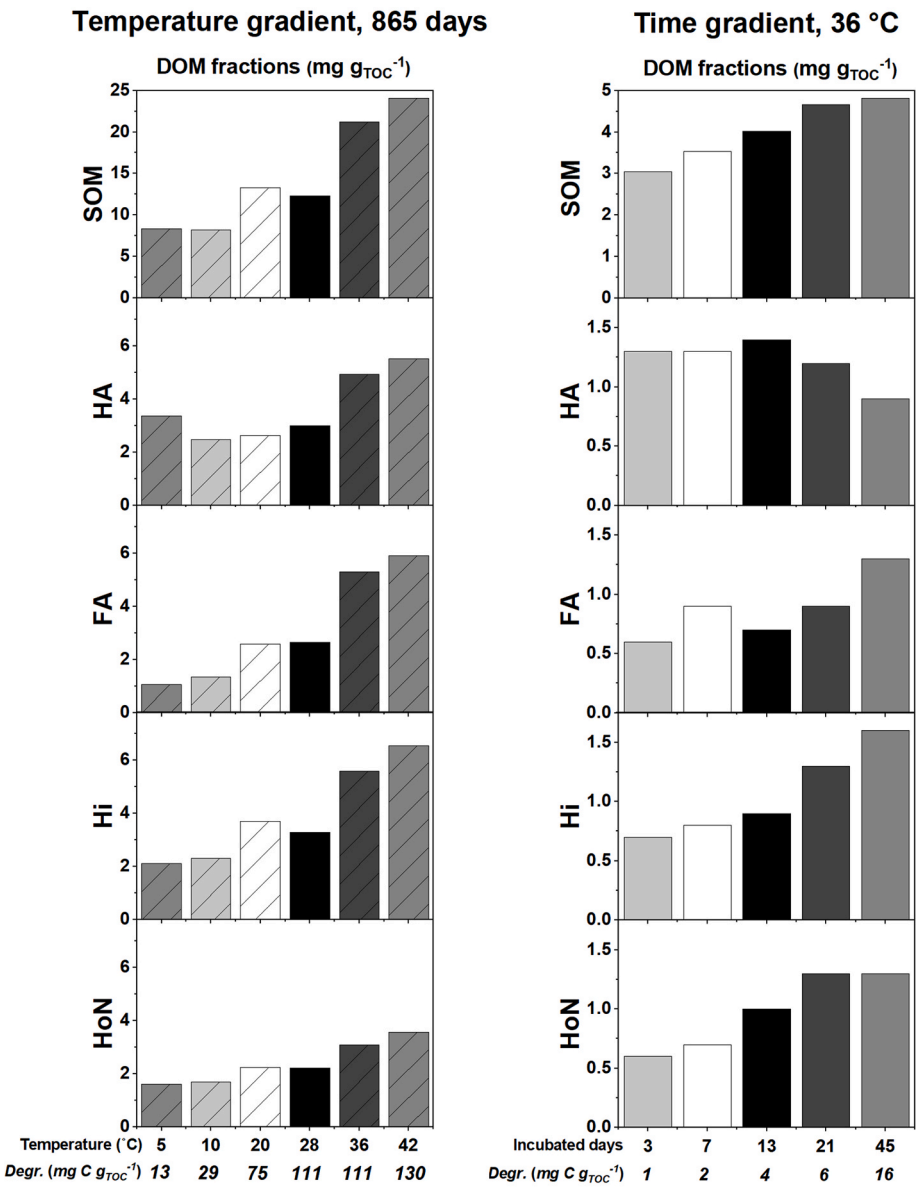

Fig. 6. Left: Water-extractable SOM fractions with different incubation temperatures (5–42 °C) after 865 days of incubation, samples taken in November 2018. Right: water-extractable SOM fractions incubated at 36 °C for different time steps (3–45 days), both for PS layers of location P7, samples taken in November 2020. Total water-extractable SOM, HA (humic acid), FA (fulvic acid), Hi (hydrophilic acids), HoN (hydrophobic neutrals) concentrations are normalised to total organic carbon (TOC). Degr. = cumulatively degraded TOC, expressed as mg C g_{TOC}^{-1} at given temperature or days.

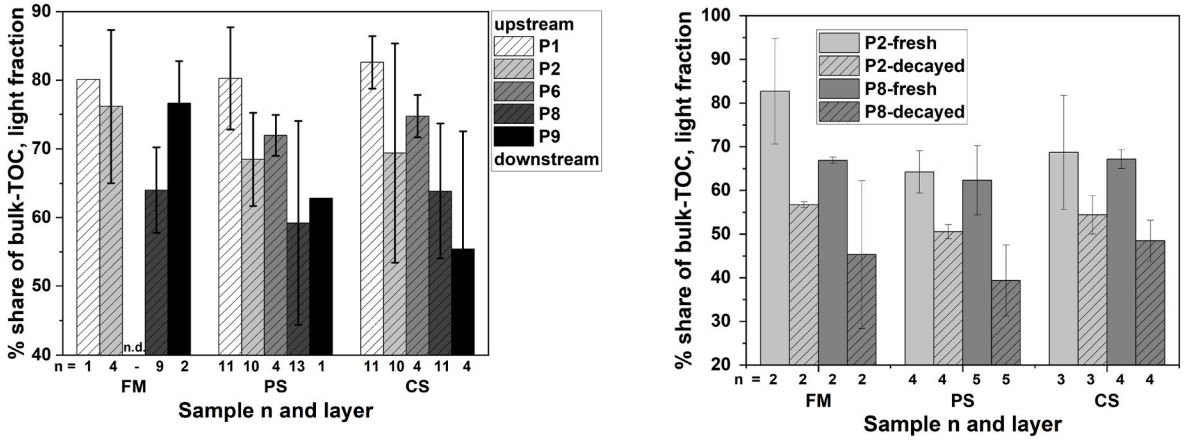

Fig. 7. Left: share of total organic carbon (TOC) in the light density fraction (< 1.4 g cm^{-3}) at different locations for FM, PS and CS layers. Right: share of total organic carbon (TOC) in the light density fraction (< 1.4 g cm^{-3}) at locations P2 and P8 for FM, PS and CS layers for fresh samples (pure bars) and decayed samples (250 days of anaerobic incubation, lined bars). For both figures: errors show standard deviation, sample n written below, samples taken in 2018 and 2019, n.d. = not determined.

This share mostly showed a decreasing trend from upstream (location P1) to downstream (location P9) for all sediment layers (Fig. 7, left), e.g. from about 80% (P1) to 55% share of bulk-TOC (P9) for CS layers. It was investigated whether the observed spatial patterns in density fractions could be caused by progressive SOM decay (ageing). Therefore, the share of TOC in the light density fraction was analysed in samples that had been incubated anaerobically in the laboratory for 250 days and compared to the density fraction distribution found for the respective sample in fresh state (i.e., straight after sampling). After 250 days, on average > 90% of degradable SOM had decayed, estimated by asymptotic curve fitting (Zander et al., 2020; Zander et al., 2022). After SOM decay in sediments from both upstream (P2) and downstream (P8) locations, a strong decrease in light density fraction TOC was found (Fig. 7, right). These results suggest that preferential decay of unbound SOM contributes to the observed pattern of a decreasing share of SOM in the light density fraction in downstream direction.

Especially at the most downstream site P9, the share of TOC in the light fraction decreased with depth (from FM to CS layers). This trend was expected, bit less obvious for the other locations. It has to be noted that dredging interventions can obfuscate sediment stratification in the investigation area.

In all samples, the decrease in light fraction TOC with SOM decay was accompanied by an enrichment in heavy carbon (^{13}C, Fig. 8, left), indicating preferential degradation of ^{12}C-containing and relative enrichment of ^{13}C-bearing components (Fig. 8, left). On average, $\delta^{13}C$ values had increased in degraded samples by 0.7‰ VPDB for upstream location P2 and by 0.6‰ VPDB for downstream location P8, compared to the respective fresh samples. Location P1, characterised by the highest SOM degradability (see grey bars Fig. 8, left), also showed the lowest $\delta^{13}C$ values of both the fresh and the decayed sample. Less pronounced differences were observed between location P2 and location P8. In field samples, sediment from location P2 to location P9 was enriched in ^{13}C compared to samples from P1, yielding a difference of about around 1‰ VPDB (Fig. 8, right). As the sample number per location comprises samples taken at several points in time, the pattern appears stable over time.

The suitability of the Rock-Eval 6© method was investigated as a further proxy to describe sediment organic matter stability/lability. The H (hydrogen) index, representing the share of the more labile (immature) organic matter, was higher at location P1 and decreased along the harbour transect (Fig. 9, top left), consistent with the trend of an increasing SOM stability. A depth gradient was not observed. The I-index (immature organic fraction) and R-index (refractory fraction or persistent SOM, both, Sebag et al., 2006) showed an inverse linear relationship with all measured samples on a single line ($R^2 = 0.998$). Upstream location P1 (triangles) showed larger I-indices and lower R-indices (Fig. 9, top right). The H-index (HI) correlated better with cumulative aerobic carbon decay after 21 days (Fig. 9, bottom right) than with the cumulative anaerobic decay after 21 days (bottom left). For one sample (location P1), the Rock-Eval 6© analysis was repeated after long-term laboratory incubation. It is seen that the organic matter decay led to a shift of the I-index and the R-index towards the less easily degradable SOM from locations P2 to P9 (Fig. 9, top right).

4. Discussion

Consistent differences in water-extractable SOM fractions, carbon stable isotope signatures and stability indices obtained from Rock-Eval 6© pyrolysis have been identified in sediment samples along an upstream -downstream gradient in the tidal river Elbe. The gradual changes in these properties are likely to originate from a gradient of upstream input of easily degradable, phytoplanktonic organic matter and corroborate the observed differences in short-term SOM decay rates (Fig. 4).

4.1. Stratification of chemical and biological indicators along the transect

Along the Elbe river, the specific concentration of Zn in the particle size fraction of < 20 µm followed a typical stratification with average values up to 850 mg Zn kg_{DW}^{-1} found in sediments upstream of Hamburg and average values of 400 mg Zn kg_{DW}^{-1} typical for sediments transported into the harbour from the North Sea by tidal pumping (Fig. 2, right). Reese et al. (2019) segregated the Elbe River sediments from upstream (river km 580) to downstream (river km 740) in four clusters by using a multi-element fingerprinting and isotopic tracer approach. According to Reese et al. (2019), sediment from river km 580 to 615 carries the fluvial signal of the Elbe River, whereas sediment from about river km 615 to 700 was described as a mixture of marine and fluvial sediment. The specific Zn concentrations found in this study confirm those findings. Compared to earlier data (Groengroeft et al., 1998), the specific Zn concentrations more than halved, by example of point P2, indicating progressive reduction of contaminants from upstream.

Given the spatial pattern of Zn in the fraction < 20 µm, it is assumed that sediments, including sediment organic matter, are dominated by the fluvial signature at location P1, while sediments from location P2 onwards (river km 619, Fig. 8, right) reached the upstream harbour area from downstream by tidal pumping (Schwartz et al., 2015) and to a lesser extent by transport from upstream to downstream. Therefore, the

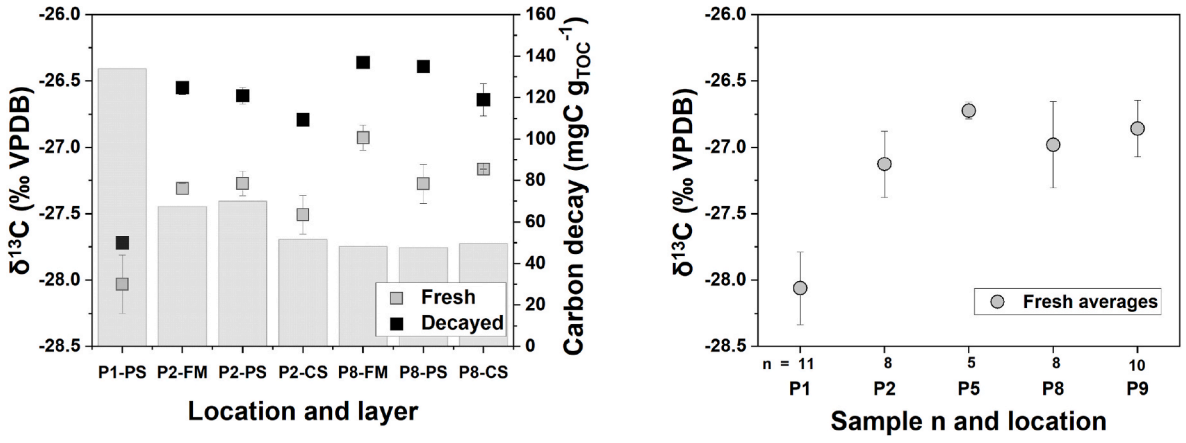

Fig. 8. Left: Averages of stable carbon isotope signatures before (fresh) and after (decayed) 250 days of anaerobic SOM decay for three sediment layers (FM, PS, CS) at location P1, P2 and P8. Samples taken in November 2018, errors show standard deviation, n = 2, grey transparent bars show total carbon decay. Right: fresh sample average stable carbon isotope signatures for FM, PS and CS layers at locations P1, P2, P5, P8 and P9, samples from 2018. Values are expressed relative to Vienna Pee Dee Belemnite (VPDB).

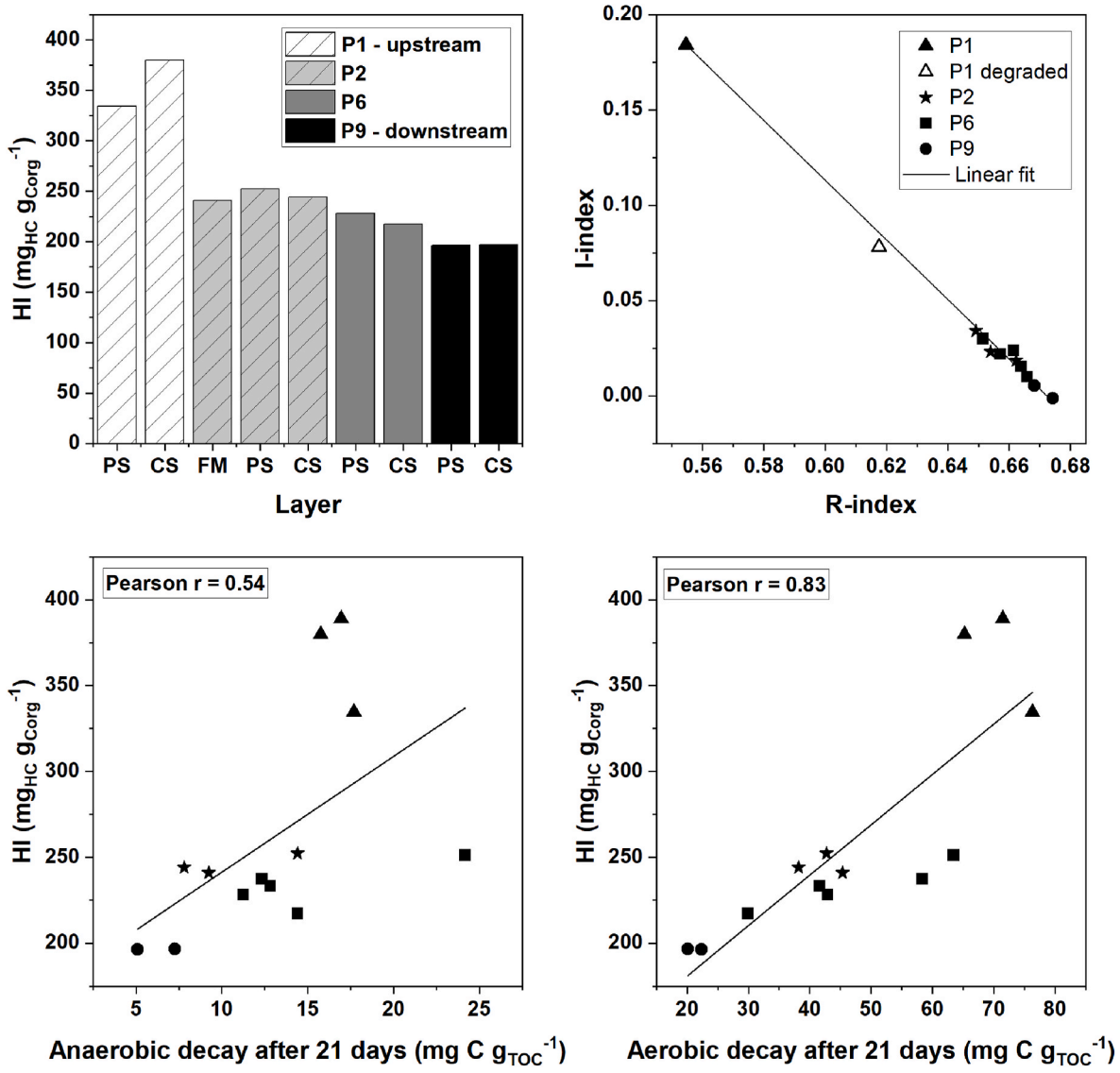

Fig. 9. Rock-Eval 6© parameters (according to Sebag et al., 2016) in fresh and degraded sediment samples. Hydrogen-index (HI, top left, samples from November 2018). I-index versus R-index (top right), Hydrogen-index versus cumulative anaerobic (bottom left) and aerobic decay after 21 days (bottom right), samples from 2018, see Table 1. All data points for fresh sediment, except for open triangle (degraded sediment from location P1). Top right legend valid for bottom panel.

properties of sediment organic matter at locations downstream of P1 not only result from the decay of upstream SOM ('age gradient') but also reflect downstream SOM transported into the investigation area and thus a source gradient. As these sediments receive less input from (upstream) fresh, easily degradable biogenic organic matter, their organic matter is older, more degraded and bound in organo-mineral complexes. This argumentation is supported by the enrichment in $\delta^{13}C$ at downstream locations (Fig. 8), a lower share of TOC in the low-density fraction (Fig. 7), and a higher ratio of acid-base over water-extractable SOM (Fig. 5 and Fig. S1).

Due to the spatial distribution of the Zn content in the fraction < 20 µm (Fig. 2) it was expected that SOM origin would be similar for all locations downstream of P2. This was supported by the fact that the I-index and the R-index for samples from P2 to P9 clustered around very similar values (high R-indices, low I-indices, Fig. 9, top right). Whereas the most upstream sample (P1) was characterised by a low R-index (persistent, old SOM) and high I-index (immature, fresh SOM). As a result of SOM degraded in this sample during long-term laboratory incubation, the relationship between immature and persistent SOM shifted towards the signature of the more downstream field samples, corroborating the H- and R-indices as being suitable for identifying labile and stable organic matter. The stability/maturity gradient was also indicated by other parameters, i.e., stable isotopes, density fractions and degradation rates, see also discussion in section 4.3.

Zander et al. (2020; 2022) showed SOM degradability to decrease from upstream to downstream locations in the Port of Hamburg. This aligned with a decrease of chlorophyll *a*, indicating an upstream driven input of fresh algal biomass (Deng et al., 2019; Schoel et al., 2014; Fig. 3), as well as a decrease in silicic acid in the sediments' pore water, indicative of a gradient in presence of siliceous biota, and a decrease in microbial biomass and extracellular polymeric substances (Fig. 3). Upstream locations are therefore characterised by higher input of easily degradable organic matter, reflected by a higher share of water-extractable hydrophilic acids that represent more easily degradable DOM (Straathof et al., 2014; Fig. 5) and a lower ratio of acid/base to water-extractable SOM compared to downstream locations (Fig. 5 and Fig. S1). The latter reflects a stronger downstream SOM binding to the sediment's mineral phase and thus a lower bioavailability of organic matter, which is in turn consistent with the downstream decreasing share of light density (i.e., non-mineral-bound) organic matter (Fig. 7).

The pronounced decline in SOM degradability from upstream to downstream locations in the Port of Hamburg further corresponded to a decline in short-term oxygen consumption (AT_{3h}, Fig. 3) from upstream to downstream locations.

It should be noted that the suggested source gradient of easily degradable SOM from upstream to downstream does not imply that upstream SOM is completely degradable. Also from the upstream catchment, a significant share of mineral-bound SOM is transported into the investigation area, evidenced by TOC in the heavy density fraction (Fig. 7, difference of light density TOC to 100%). Further, SOM degradation kinetics indicate > 60% of TOC to be present in the recalcitrant (non-degradable) fraction (Zander et al., 2022).

4.2. Organic matter lability: Chemical organic matter (SOM) fractions

According to Bongiorno et al. (2019), hydrophilic SOM (Hi) mainly comprises the soluble fractions of total organic carbon (TOC), primarily composed of root and microbial exudates and products of hydrolysis and leachates of SOM. In the investigated sediments, the hydrophilic SOM fraction (Hi) correlated strongly positively with the share of easily degradable organic matter, represented by mass of sediment in the light density fraction and negatively with mineral-bound organic matter (heavy density fraction, not shown). Hydrophilic compounds such as carbohydrates, organic acids and proteins provide a readily available carbon source to the microbial community (Marschner and Kalbitz, 2003; Battin et al., 2008; Straathof et al., 2014). It is therefore assumed that along the investigated gradient the Hi fraction can be regarded as an indicator for labile organic matter, present in higher concentrations due to biogenic input (as discussed above) at upstream locations (water--extraction, Fig. 5, left). In this study, the Hi concentration dropped with decreasing organic matter lability (increasing stabilization) along the transect, which matches the findings of Straathof et al. (2014).

The decreasing share of water-extractable SOM from upstream to downstream (Fig. 5, left) is assumed to be related to (1) the progressive decay of fresh organic matter, namely, less strongly bound to the mineral phase, as the sediment travels along the transect (age gradient), and to (2) the higher input of easily degradable organic matter upstream (source gradient), evidenced by higher upstream chlorophyll concentrations, higher microbial biomass, silicic acid and EPS (Table 1). This interpretation implies that SOM originating from downstream sources *a priori* contains less hydrophilic SOM. The evolution of water-extractable SOM, measured in laboratory incubations, corroborated the marked spatial trends observed in the field, showing concentrations to increase as a result of and proportional to progressive SOM decay as detected by gas phase CH_4 and CO_2 concentrations. The latter were the main pathway for carbon released by microbial SOM degradation, exceeding carbon released as DOM by a factor of five.

In comparison to labile hydrophilic SOM compounds, hydrophobic SOM compounds (particularly fulvic acids, FA, and hydrophobic neutrals, HoN) have been associated with lower carbon turnover rates (Straathof et al., 2014). This was also seen in this study as the share of FA and HoN increased with decreasing organic matter degradability from upstream to downstream locations (Fig. S1, left). These more hydrophobic components are assumed to represent the less-easily degradable SOM fraction which undergoes little change in the short or intermediate term (i.e., during the time of sediment organic matter transport from upstream to downstream). The results clearly indicate the different composition of SOM along the transect.

The increasing ratio between acid-base and water-extractable SOM from upstream to downstream (Fig. 5, right) is consistent with the higher share of mineral bound SOM downstream. The mineral-bound SOM is considered to be more strongly protected against microbial SOM decay, but is liberated by the acid-base-extraction. Upstream, the share of water-extractable SOM was higher, hence less SOM was bound to the mineral phase than at more downstream locations, corroborating the results from the density fractionation presented in section 3.3 (see also later section 4.3). The ratio of Hi liberated by the acid-base-extraction to Hi in the water extractable fraction was highest for the most downstream location P9. This finding supports the concept that the Hi fraction in solution is preferably degraded and therefore detected less in the water-extractable fraction at sites with less input of fresh organic matter (i.e., dominated by older organic matter, Fig. 5, right). At location P9, Hi still represents a minor share of about 20% of the sediment-bound organic matter, which is dominated by the humic (HA, FA and HON) SOM fractions (Fig. 5, middle). Downstream locations were characterized by more mineral-bound SOM, seen by the increasing concentration of hardly soluble, acid-base extractable total SOM fractions along the transect. This interpretation is further confirmed by the downstream increasing contribution of the heavy density SOM fraction (Fig. 7).

In the absence of data on water-extractable or acid-base-extractable SOM from fluviatile sediments, data from soils and compost are used for comparison. Bongiorno et al. (2019) reported a share of water-extractable SOM between 0.06% and 0.40% of TOC for European soils. Lundquist et al. (1999) and Haynes (2005) found between 0.05% and 0.40% of TOC for agricultural African soils, and Straathof et al. (2014) reported 0.09% and 0.61% of TOC for composts. In this study, compared with the literature above, relatively high values of water-extractable SOM were found, i.e. between 0.2% and 1.2% of TOC, in line with previous observations that HA and FA in natural aquatic samples were composed of smaller source molecules (Schellekens et al., 2017).

4.3. Physical organic matter fractions and stable carbon isotopes

At downstream locations, a greater share of organic matter was associated with the mineral phase, reflecting in a larger share of organic carbon in the heavy density fraction, thus reducing SOM accessibility to degradation (Baldock and Skjemstad 2000; Six and Paustian 2014; Gao et al., 2019). Positive correlations were seen between the share of sediment in the light density fraction and water-extractable SOM fractions HA, FA and (less) HoN as well as with silicic acid and microbial biomass. For water-extractable hydrophilics (Hi), strong correlations were not observed, assuming that this might be the result of the rapid degradation of water-extractable Hi. Also Schartau et al. (2019) found organic matter in suspended matter in the coastal zone of the German Bight, into which the Elbe river discharges, to be dominated by mineral bound organic matter and hence also by the properties of the mineral phase, continuing the trend observed for settled sediments in this study. Shares of fresh, non-mineral bound organic matter only increased towards the pelagic zone again.

Sedimentary $\delta^{13}C$ values result from the $\delta^{13}C$ signature of the multiple organic carbon sources contributing to the sediment organic matter. $\delta^{13}C$ values between −26 and −28‰ VPDB align with the signature of terrestrial soils (Nordt and Holliday, 2017) which contain already stabilized organic matter, but also with $\delta^{13}C$ values measured for phyto- and zooplankton (Zeng et al., 2010; Harmelin-Vivien et al., 2010). Higher enrichment of ^{13}C in sediment from locations downstream of P1 is consistent with a higher extent of SOM stabilization, and strengthening the hypothesis of predominance of more degraded and hence more recalcitrant remaining organic matter at downstream locations, as also evidenced by lower degradation rates (Zander et al., 2020). The relationship between ^{13}C-enriched and degraded SOM was corroborated by higher concentrations of ^{13}C found in the SOM after long-term (> 500 days) decay in the laboratory (enrichment in $\delta^{13}C$, Fig. 8, left), indicating the preferential decay of ^{12}C-containing SOM constituents and is consistent with the depth gradients found in terrestrial soils (e.g. Acton et al., 2013; Brunn et al., 2014; Wang et al., 2015). SOM at location P1 (Fig. 8, left) showed the highest decay rates but the lowest shift towards ^{13}C concentrations. This observation could be explained by the fact that the extent of isotopic fractionation declines with increasing reaction rates (Chanton et al., 2008; Gebert and Streese-Kleeberg, 2017).

The low upstream $\delta^{13}C$ values (Fig. 8, left), indicative of higher

shares of labile SOM and lower shares of stabilized SOM, supported the first hypothesis of fresh planktonic, more degradable biomass feeding the organic matter stocks from upstream, in downstream direction progressively 'diluted' with more stable organic matter. An (expected) enrichment of $\delta^{13}C$ with depth was not found (Fig. 8, left), which may be related to the fact that the samples shown in Fig. 8 (right) were taken at the end of the year (November). The main sedimentation events occur in the summer months, implying that the sampled material had already undergone partial depletion of the most degradable SOM throughout the year, possibly leading to a similar isotopic signature than found for the layer underneath. Moreover, direct comparison of depth-related phenomena assumes that the deposited material does not vary over time and that dredging interventions do not disturb the profile. For both reasons, conclusions relying on the assumptions of an intact depth profile have to be drawn with reservation.

The upstream-downstream decreasing trend of the Hydrogen-index (HI) (Fig. 9), representing the easily degradable SOM (Sebag et al., 2016), was in line with the trends of SOM degradability (Zander et al., 2020), the extractable SOM fractions (Fig. 5) and the stable carbon isotope signatures (Fig. 8). Larger I-indices and lower R-indices, as found at location P1, are indicative of more labile biological compounds (Sebag et al., 2016). Sebag et al. (2016) analysed > 1300 samples with the Rock-Eval 6© method and plotted the immature organic fraction representing I-index and the persistent SOM representing R-index. Compared to the identified relationships in that paper, the ratio of I-index and R-index found in this study was comparable to A-horizons of Leptosols/Ferralsols and B-horizons of Cambisols. Location P1 showed the most similar R-indices and I-indices to A and Bh-horizons. The ratio of I-indices to R-indices of the harbour sediments of this study are best represented by those found for organo-mineral horizons by Sebag et al. (2016). This supported the findings that larger shares of SOM at downstream locations are indeed found in the heavy density fraction (at most locations > 50% DM-bulk, Table 1). Positive correlations between short-term respiration after 21 days (R21) and the Rock-Eval 6© parameters Hydrogen-index and I-index reveal that both can serve as a proxy for the more easily degradable organic matter in these sediments. Further, the connection between these two approaches of classification of OM lability was shown.

5. Conclusions

In the investigated transect within the tidal Elbe river, sediment-bound organic matter is imported both from downstream as well as from upstream areas whereas fresh, labile organic matter enters the system from upstream, as indicated by the gradients in chlorophyll *a* and silicic acid. The gradient in the specific Zn concentration in the particle size fraction < 20 μm indicated showed that the upstream location P1 being nourished primarily from upstream fluviatile sediments while the other locations carried a stronger downstream signature. The decreasing SOM degradability from upstream to downstream was accompanied by an increasing share of SOM bound in organo-mineral associations. This was evidenced by lower shares of SOM detected in the light density fraction, enrichment in ^{13}C, a higher ratio of acid-base to water-extractable SOM and lower Hi-indices.

The decrease in concentrations of biological parameters (i.e., chlorophyll *a*, microbial biomass, silicic acid, EPS and oxygen consumption) indicated a change in organic matter composition from upstream to downstream. SOM lability decreased from upstream to downstream, evidenced by an increased share of total SOM found in the acid-base-extractable fractions downstream. The proposed gradient of SOM lability is corroborated by the decrease of carbon in the light density fractions in sediments with older, more decayed and hence stabilized organic matter, and from upstream to downstream. The enrichment of ^{13}C in the organic matter at downstream locations also confirmed a higher extent of decay, strengthening the hypothesis of already degraded organic matter dominating at downstream locations. This study further confirmed this hypothesis by the large enrichment of ^{13}C in laboratory-decayed sediment samples. Thermometric pyrolysis (Rock-Eval 6©) further confirmed the trends indicated by the stable carbon isotope signatures and patterns in extractable SOM fractions. The Hydrogen-index related well to SOM decay rates. The relationship between I- and R-index supported the findings that a significant share of downstream SOM is bound in organo-mineral complexes. These RE6 indices may therefore serve as powerful proxies for SOM lability/stability in river and estuarine sediments.

Potential products of SOM decay (i.e., Hi, FA, HA and total water-extractable fraction) correlated with the SOM decay rates. Larger concentrations of water-extractable SOM fractions were found with increasing temperature and/or increasing incubation time, confirming the assumption that these compounds represent products rather than sources of SOM decay.

Declaration of competing interest

The authors declare the following financial interests/personal relationships which may be considered as potential competing interests: Julia Gebert reports financial support and equipment, drugs, or supplies were provided by Hamburg Port Authority AöR.

Data availability

Data will be made available on request.

Acknowledgements

This study was funded by Hamburg Port Authority AöR and carried out within the project BIOMUD, a member of the MUDNET academic network www.tudelft.nl/mudnet/. Carbon contents in density fractions and stable isotopes were measured by the Institute of Soil Science (Prof Dr Annette Eschenbach, Dr Alexander Gröngröft and Dr Christian Knoblauch, respectively). Rock-Eval 6© analyses were performed by Deltares through Dr Martine Kox.

Appendix A. Supplementary data

Supplementary data to this article can be found online at https://doi.org/10.1016/j.apgeochem.2023.105760.

References

Acton, P., Fox, J., Campbell, E., Rowe, H., Wilkinson, M., 2013. Carbon isotopes for estimating soil decomposition and physical mixing in well-drained forest soils. Journal of Geophysical Research-Biogeosciences 118 (4), 1532–1545. https://doi.org/10.1002/2013JG002400.

Ankit, A., Muneer, W., Gaye, B., Lahajnar, N., Bhattacharya, S., Bulbul, M., Jehangir, A., Anoop, A., Mishra, P.K., 2022. Apportioning sedimentary organic matter sources and its degradation state: inferences based on aliphatic hydrocarbons, amino acids and δ15N. Environ. Res. 205, 112409 https://doi.org/10.1016/j.envres.2021.112409.

Arndt, S.B., Jørgensen, B.B., LaRowe, D.E., Middelburg, J.J., Pancost, R.D., Regnier, P., 2013. Quantifying the degradation of organic matter in marine sediments: a review and synthesis. Earth Sci Reviews 123, 53–58. https://doi.org/10.1016/j.earscirev.2013.02.008.

Bastviken, D., Olsson, M., Tranvik, L., 2003. Simultaneous measurements of organic carbon mineralization and bacterial production in oxic and anoxic lake sediments. Microb. Ecol. 46, 73–82. https://doi.org/10.1007/s00248-002-1061-9.

Battin, T.J., Kaplan, L.A., Findlay, S., Hopkinson, C.S., Marti, E., Packman, A.I., Newbold, J.D., Sabater, F., 2008. Biophysical controls on organic carbon fluxes in fluvial networks. Nat. Geosci. 1, 95–100.

Bongiorno, G., Bünemann, E.K., Oguejiofor, C.U., Meier, J., Gort, G., Comans, R., Mäder, P., Brussaard, L., de Goede, R., 2019. Sensitivity of labile carbon fractions to tillage and organic matter management and their potential as comprehensive soil quality indicators across pedoclimatic conditions in Europe. Eco Indic 99, 38–50.

Brunn, M., Spielvogel, S., Sauer, T., Oelmann, Y., 2014. Temperature and precipitation effects on $\delta^{13}C$ depth profiles in SOM under temperate beech forests. Geoderma 235–235, 146–153. https://doi.org/10.1016/j.geoderma.2014.07.007.

Catalán, N., Marcé, R., Kothawala, D.N., Tranvik, L.J., 2016. Organic carbon decomposition rates controlled by water retention time across inland waters. Nat. Geosci. 9, 501–504. https://doi.org/10.1038/ngeo2720.

Chanton, J.P., Powelson, D.K., Abichou, T., Fields, D., Green, R., 2008. Effect of temperature and oxidation rate on carbon-isotope fractionation during methane oxidation by landfill cover materials. Environ. Sci. Technol. 42, 7818–7823.
Deng, Z., He, Q., Safar, Z., Chassagne, C., 2019. The role of algae in fine sediment flocculation: in-situ and laboratory measurements. Mar. Geol. 413, 71–84.
DIN EN ISO 14240-2:2011-09. Soil quality - Determination of soil microbial biomass - Part 2: Fumigation-extraction method (ISO 14240-2:1997).
DIN 38404, 2012. German Standard Methods for the Examination of Water, Waste Water and Sludge - Physical and Physico-Chemical Parameters (Group C) - Calculation of the Calcit Saturation of Water. Beuth, Berlin, Germany.
DIN 38405, 1990. German Standard Methods for the Examination of Water, Waste Water and Sludge; Anions (Group D); Determination of Dissolved Silicate by Spectrometry (D 21). https://doi.org/10.1016/B978-0-12-405940-5.00007-8. Beuth, Berlin, GermanyDittmar, T. 2015. Reasons Behind the Long-Term Stability of Dissolved Organic Matter. Biogeochemistry of Marine Dissolved Organic Matter.
DIN EN 1484, 1997. Water Analysis - Guidelines for the Determination of Total Organic Carbon (TOC) and Dissolved Organic Carbon (DOC). Beuth, Berlin, Germany.
DIN EN 15933, 2012. Sludge, Treated Biowaste and Soil - Determination of pH. Beuth, Berlin, Germany.
DIN EN 16168, 2012. Sludge, Treated Biowaste and Soil - Determination of Total Nitrogen Using Dry Combustion Method. Beuth, Berlin, Germany.
DIN EN 27888, 1993. Water Quality; Determination of Electrical Conductivity. Beuth, Berlin, germany.
DIN ISO 10304, 2009. Water Quality - Determination of Dissolved Anions by Liquid Chromatography of Ions - Part 1: Determination of Bromide, Chloride, Fluoride, Nitrate, Nitrite, Phosphate and Sulfate. Beuth, Berlin, Germany.
DIN ISO 10694, 1995. Soil Quality - Determination of Organic and Total Carbon after Dry Combustion (Elementary Analysis). Beuth, Berlin, Germany.
DIN ISO 11277, 2009. Soil Quality - Determination of Particle Size Distribution in Mineral Soil Material - Method by Sieving and Sedimentation. Beuth, Berlin, Germany.
DIN ISO 11465, 1993. Soil Quality - Determination of Dry Matter and Water Content on a Mass Basis - Gravimetric Method. Beuth, Berlin, Germany.
DIN ISO 11732, 2005. Water Quality - Determination of Ammonium Nitrogen - Method by Flow Analysis (CFA and FIA) and Spectrometric Detection. Beuth, Berlin, Germany.
DIN ISO 6878, 2004. Water Quality - Determination of Phosphorus - Ammonium Molybdate Spectrometric Method. Beuth, Berlin, Germany.
FGG Elbe data portal, 2020. https://www.elbe-datenportal.de/. (Accessed 18 April 2020).
Gebert, J., Streese-Kleeberg, J., 2017. Coupling stable isotope analysis with gas push-pull tests to derive in situ values for the fractionation factor aox associated with the microbial oxidation of methane in soils. Soil Sci. Soc. Am. J. 81, 1107–1114. https://doi.org/10.2136/sssaj2016.11.0387.
Gebert, J., Köthe, H., Gröngröft, A., 2006. Prognosis of methane formation by River Sediments. J. Soils Sediments 6 (2), 75–83.
Grasset, S., Moras, S., Isidorova, A., Couture, R.-M., Linkhorst, A., Sobek, S., 2021. An empirical model to predict methane production in inland water sediment from particular organic matter supply and reactivity. Limnol. Oceanogr. 9999, 1–13. https://doi.org/10.1002/lno.11905.
Groengroeft, A., Jaehnig, U., Miehlich, G., Lueschow, R., Maass, V., Stachel, B., 1998. Distribution of metals in sediments of the Elbe estuary in 1994. Water Sci. Technol. 37, 109–116. https://doi.org/10.1016/S0273-1223(98)00189-9.
Harmelin-Vivien, M., Dierking, J., Bănaru, D., Fontaine, M.F., Arlhac, D., 2010. Seasonal variation in stable C and N isotope ratios of the rhone river inputs to the mediterranean Sea (2004–2005). Biogeochemistry 100, 139–150. http://www.jstor.org/stable/40800614.
Haynes, R.J., 2005. Labile organic matter fractions as central components of the quality of agricultural soils: an overview. Adv. Agron. 85, 221–268.
Helfrich, M., Flessa, H., Mikutta, R., Dreves, A., Ludwig, B., 2007. Comparison of chemical fractionation methods for isolating stable soil organic carbon pools. Eur. J. Soil Sci. 58, 1316–1329.
Hoffland, E., Kuyper, T.W., Comans, R.N.J., Creamer, R.E., 2020. Eco-functionality of organic matter in soils. Plant Soil 455, 1–22. https://doi.org/10.1007/s11104-020-04651-9.
Jommi, C., Murano, S., Trivellato, E., Zwanenburg, C., 2019. Experimental results on the influence of gas on the mechanical response of peats. Geotechnique 69 (9), 753–766. https://doi.org/10.1680/jgeot.17.P.148.
Kobierski, M., Banach-Szott, M., 2022. Organic matter in riverbank sediments and fluvisols from the flood zones of lower vistula river. Agronomy 2022 12, 536. https://doi.org/10.3390/agronomy12020536.
Kögel-Knabner, I., Rumpel, C., 2018. Advances in molecular approaches for understanding soil organic matter composition, origin, and turnover: a historical overview. Adv. Agron. 149, 1–48. https://doi.org/10.1016/bs.agron.2018.01.003.
Lafargue, E., Marquis, F., Pillot, D., 1998. Rock-Eval 6 applications in hydrocarbon exploration, production, and soil contamination studies. Oil Gas Sci. Technol. 53 (4), 421–437.
Lehmann, J., Kleber, M., 2015. The contentious nature of soil organic matter. Nature 528. https://doi.org/10.1038/nature16069.
Lundquist, E.J., Jackson, L.E., Scow, K.M., 1999. Wet-dry cycles affect dissolved organic carbon in two California agricultural soils. Soil Biol. Biochem. 31, 1031–1038.
Marschner, B., Kalbitz, K., 2003. Controls of bioavailability and biodegradability of dissolved organic matter in soils. Geoderma 113, 211–235.
Meijboom, F.W., Hassink, J., van Noordwijk, M., 1995. Density fractionation of soil macroorganic matter using silica suspensions. Soil Biol. Biochem. 27, 1109–1111.
Nordt, L.C., Holliday, V.T., 2017. Stable carbon isotopes in soils. In: Gilbert, A.S. (Ed.), Encyclopedia of Geoarchaeology. Encyclopedia of Earth Sciences Series. Springer, Dordrecht. https://doi.org/10.1007/978-1-4020-4409-0_13.
Oliveira, B.R.F., Smit, M.P.J., van Paassen, L.A., Grotenhuis, J.T.C., Rijnaarts, H.H.M., 2017. Functional properties of soils formed from biochemical ripening of dredged sediments—subsidence mitigation in delta areas. J. Soils Sediments 17, 286–298. https://doi.org/10.1007/s11368-016-1570-7.
Olk, D.C., Bloom, P.R., Perdue, E.M., Chen, Y., McKnight, D.M., Farenhorst, A., Senesi, N., Chin, Y.-P., Schmitt-Koplin, P., Hertkorn, N., Harir, M., 2019. Environmental and agricultural relevance of humic fractions extracted by alkali from soils and natural waters. J. Environ. Qual. 48, 217–232. https://doi.org/10.2134/jeq2019.02.0041.
Reese, A., Zimmermann, T., Pröfrock, D., Irrgeher, J., 2019. Extreme spatial variation of Sr, Nd and Pb isotopic signatures and 48 element mass fractions in surface sediment of the Elbe River Estuary - suitable tracers for processes in dynamic environments? Sci. Total Environ. 668, 512–523.
Schartau, M., Riethmüller, R., Flöser, G., van Beusekom, J.E.E., Krasemann, H., Hofmeister, R., Wirtz, K., 2019. On the separation between inorganic and organic fractions of suspended matter in a marine coastal environment. Prog. Oceanogr. 171, 231–250. https://doi.org/10.1016/j.pocean.2018.12.011.
Schellekens, J., Buurman, P., Kalbitz, K., van Zomeren, A., Vidal-Torradoa, P., Cerli, C., Comans, R.N.J., 2017. Molecular features of humic acids and fulvic acids from contrasting environments. Environ. Sci. Technol. 51, 1330–1339. https://doi.org/10.1021/acs.est.6b03925.
Schoel, A., Hein, B., Wyrwa, J., Kirchesch, V., 2014. Modelling water quality in the Elbe and its estuary –large scale and long term applications with focus on the oxygen budget of the estuary. Die Kueste 81, 203–232.
Schwartz, R., Eichweber, G., Entelmann, I., Keller, I., Rickert-Niebuhr, K., Röper, H., Wenzel, C., 2015. Aspects of Pollutant Sediment Management in the Tidal Elbe. HW, vol. 59. https://doi.org/10.5675/HyWa_2015,6_9. H.6.
Sebag, D., Disnar, J.-R., Guillet, B., Di Giovanni, C., Verrecchia, E.P., Durand, A., 2006. Monitoring organic matter dynamics in soil profiles by 'Rock-Eval pyrolysis': bulk characterization and quantification of degradation. Eur. J. Soil Sci. 57 (3), 344–355.
Sebag, D., Verrecchia, E.P., Cécillon, L., Adatte, T., Albrecht, R., Aubert, M., Bureau, F., Cailleau, G., Copard, Y., Decaens, T., Disnar, J.-R., Hetényi, M., Nyilas, T., Trombino, L., 2016. Dynamics of soil organic matter based on new Rock-Eval indices. Geoderma 284, 185–203.
Serviceportal, Hamburg, 2020. HamburgService – Wassergüte-Auskunft. https://gateway.hamburg.de/hamburggateway/fvp/fv/BSU/wasserguete/wfWassergueteAnfrageListe.aspx?Sid=37#. (Accessed 11 March 2020).
Shakeel, A., Kirichek, A., Chassagne, C., 2019. Is density enough to predict the rheology of natural sediments? Geo Mar. Lett. 39, 427–434. https://doi.org/10.1007/s00367-019-00601-2.
Shakeel, A., Kirichek, A., Talmon, A., Chassagne, C., 2021. Rheological analysis and rheological modelling of mud sediments: what is the best protocol for maintenance of ports and waterways? Estuar. Coast Shelf Sci. 257, 107407.
Shen, Q., Suarez-Abelenda, M., Camps-Arbestain, M., Pereira, R.C., McNally, S.R., Kelliher, F.M., 2018. An investigation of organic matter quality and quantity in acid soils as influenced by soil type and land use. Geoderma 328, 44–55.
Sills, G.C., Gonzalez, R., 2001. Consolidation of naturally gassy soft soil. Geotechnique 51 (7), 629–639.
Song, B., Niu, S., Zhang, Z., Yang, H., Li, L., Wan, S., 2012. Light and heavy fractions of soil organic matter in response to climate warming and increased precipitation in a temperate steppe. PLoS One 7, e33217. https://doi.org/10.1371/journal.pone.0033217.
Straathof, A.L., Chincarini, R., Comans, R.N.J., Hoffland, E., 2014. Dynamics of soil dissolved organic carbon pools reveal both hydrophobic and hydrophilic compounds sustain microbial respiration. Soil Biol. Biochem. 79, 109–116.
Van den Pol-van Dasselaar, A., Oenema, O., 1999. Methane production and carbon mineralisation of size and density fractions of peat soils. Soil Biol. Biochem. 31, 877–886.
Van Zomeren, A., Comans, R.N.J., 2007. Measurement of humic and fulvic acid concentrations and dissolution properties by a rapid batch procedure. Environ. Sci. Technol. 41, 6755–6761.
Vance, E.D., Brookes, P.C., Jenkinson, D.S., 1987. An extraction method for measuring soil microbial biomass C. Soil Biol. Biochem. 19, 703–707. https://doi.org/10.1016/0038-0717(87)90052-6.
Vannote, R.L., Minshall, W.G., Cummins, K.W., Sedell, J.R., Cushing, C.E., 1980. The river continuum concept. Can. J. Fish. Aquat. Sci. 37, 130–137.
Von Lützow, M., Kögel-Knabner, I., Ekschmitt, K., Flessa, H., Guggenberger, G., Matzner, E., Marschner, B., 2007. SOM fractionation methods: relevance to functional pools and to stabilization mechanisms. Soil Biol. Biochem. 39, 2183–2207.
Wakeham, S.G., Canuel, E.A., 2016. The nature of organic carbon in density-fractionated sediments in the Sacramento-San Joaquin River Delta (California). Biogeosciences 13, 567–582.
Wang, G., Jia, Y., Li, W., 2015. Effects of environmental and biotic factors on carbon isotopic fractionation during decomposition of soil organic matter. Sci. Rep. 5, 11043.
Ward, N.D., Bianchi, T.S., Medeiros, P.M., Seidel, M., Richey, J.E., Keil, R.G., Sawakuchi, H.O., 2017. Where carbon goes when water flows: carbon cycling across the aquatic continuum. Front. Mar. Sci. 4, 7. https://doi.org/10.3389/fmars.2017.00007.
Wei, J.E., Chen, Y., Wang, J., Yan, S.-B., Zhang, H.-H., Yang, G.-P., 2021. Amino acids and amino sugars as indicators of the source and degradation state of sedimentary

organic matter. Mar. Chem. 230, 103931 https://doi.org/10.1016/j.marchem.2021.103931.
Westrich, J.T., Berner, R.A., 1984. The role of sedimentary organic matter in bacterial sulfate reduction: the G model tested. Limnol. Oceanogr. 29 (2), 236–249.
Wingender, J., Strathmann, M., Rode, A., Leis, A., Flemming, H.C., 2001. Isolation and biochemical characterization of extracellular polymeric substances from Pseudomonas aeruginosa. Methods Enzymol. 336, 302–314.
Wurpts, R., Torn, P., 2005. 15 Years experience with fluid mud: definition of the nautical bottom with rheological parameters. Terra Aqua (Engl. Ed.) 99.
Zander, F., 2022. Turnover of Suspended and Settled Organic Matter in Ports and Waterways. Doctoral thesis. Delft University of Technology. https://doi.org/10.4233/uuid:f4d57842-9603-41aa-950b-1009ab3c3fe3.
Zander, F., Heimovaara, T., Gebert, J., 2020. Spatial variability of organic matter degradability in tidal Elbe sediments. J Soil Sediments. Special issue. https://doi.org/10.1007/s11368-020-02569-4.
Zander, F., Groengroeft, A., Eschenbach, A., Heimovaara, T.J., Gebert, J., 2022. Organic matter pools in sediments of the tidal Elbe river. Limnologica 96. https://doi.org/10.1016/j.limno.2022.125997.
Zeng, Q., Kong, F., Tan, X., Wu, X., 2010. Variations and relationships of stable isotope composition in size-fractionated particulate organic matter. Pol. J. Environ. Stud. 19, 1361–1367.